ISBN: 978-3-95450-202-8 doi:10.18429/JACoW-HB2018-THA2WE02

APPLICATION OF MACHINE LEARNING FOR THE IPM-BASED PROFILE RECONSTRUCTION

M. Sapinski*, R. Singh, D. Vilsmeier,
GSI Helmholtzzentrum für Schwerionenforschung, 64291 Darmstadt, Germany
J. Storey, CERN, 1211 Geneva 23, Switzerland

Abstract

One of the most reliable devices to measure the transverse beam profile in hadron machines is Ionization Profile Monitor (IPM). This type of monitor can work in two main modes: collecting electrons or ions. Typically, for lower intensity beams, the ions produced by ionization of the residual gas are extracted towards a position-sensitive detector. Ion trajectories follow the external electric field lines, however the field of the beam itself also affects their movement leading to a deformation of the observed beam profile. Correction methods for this case are known. For high brightness beams, IPM configuration in which electrons are measured, is typically used. In such mode, an external magnetic field is usually applied in order to confine the transverse movement of electrons. However, for extreme beams, the distortion of the measured beam profile can occur. The dynamics of electron movement is more complex than in case of ions, therefore the correction of the profile distortion is more challenging. Investigation of this problem using a dedicated simulation tool and machine learning algorithms lead to a beam profile correction methods for electron-collecting IPMs.

INTRODUCTION

Ionization Profile Monitors (IPM) are devices designed to measure beam profile by extracting and detecting the position of the products of the rest gas ionization by the beam. In the most common configuration ions are extracted by external, uniform electric field. In another configuration, more adapted to high brightness beams, electrons are extracted and additional magnetic field is applied to confine their transverse displacement. There is a rich literature related to Ionization Profile Monitors, and one of the best collection of references can be found in [1].

The deformation of the beam profile registered in ion-based IPMs due to beam space charge was investigated in a series of publications [2–5]. The first three publications focus on derivation of a formula, which links the measured and the real sigma of the transverse beam distribution. The most recent formula [4], based on analytical considerations and simulations, is shown in Eq. 1. The coefficients C_1, p_1 are found by fitting the data and N is bunch population.

$$\sigma_{meas} = \sigma_{real} + C_1 N \sigma_{real}^{p_1} \quad (1)$$

The most recent work [5] proposes a method to not only correct beam sigma, but to reconstruct the original distribution of the beam, based on an iterative correction procedure. It is demonstrated, on simulations, that this method is convergent for generalized gaussian distribution.

The electron-collecting IPMs with magnetic field in the range 0.05 T to 0.2 T are successfully used in many machines in Fermilab, BNL, CERN and J-PARC. A significant distortion of the observed beam profile were reported for LHC beams [6]. This beam is smaller and the maximum bunch field higher than in other hadron machines. A comparison of various beam with respect to the space-charge conditions is shown in Fig. 1. Next frontier are electron machines, especially XFELs, where beam size can be as small as 5 μm and the bunch electric field can reach 10^8 V/m.

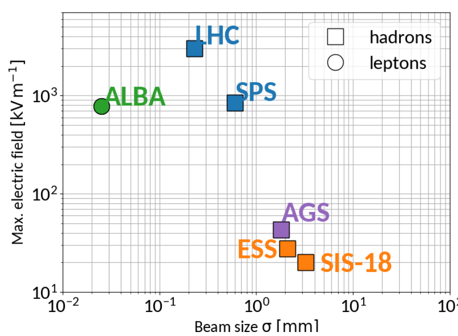

Figure 1: Comparison of typical maximum bunch electric field and beam size for various machines.

SIMULATION TOOLS

Over the years many researchers prepared their own simulation codes to track electron or ion movement in the presence of constant extraction fields and transient bunch fields [7]. These codes are often private, applicable to specific devices, lack maintenance and modern coding. Therefore, we have decided to write a new code, attempting to make it as universal as possible, modern and modular. The program, called Virtual-IPM, is written in python and is available publicly at gitlab.com and in Python Package Index [8].

In the following we will show results of simulation performed using Virtual-IPM. Because of its high space-charge effect we focus on LHC beam, with parameters given in Table 1. The assumed IPM parameters correspond to the devices used in LHC and SPS, except the position resolution, which was adopted from a new device currently being tested on CERN PS [9]. The original LHC IPM position resolution is about 150 μm, and this is not enough to observe the details of the distorted profile. We preferred to apply our analysis to the best currently available technology than to use purely

* m.sapinski@gsi.de

ISBN: 978-3-95450-202-8 doi:10.18429/JACoW-HB2018-THA2WE02

theoretical profiles. The values of adequate IPM parameters are listed in Table 2.

Table 1: LHC Beam Parameters Used as Benchmark Example

Parameter	Range
particle type	protons
σ_x	0.23 mm
σ_y	0.27 mm
$4 \cdot \sigma_z$	1.1 ns
N_{bunch}	1.4×10^{11}
bunch spacing	25 ns
E_{beam}	6.5 TeV

Table 2: Assumed IPM Parameters

Parameter	Range
distance between electrodes (d)	85 mm
extraction field E	48 kV/m
magnetic field B	0.2 T
position resolution	55 µm

In the next section we will examine various IPM configurations, as in decision process for a new device design. We use the following coordinate system: x - axis of the beam profile, y - direction of the extraction fields, z - beam direction.

ION DYNAMICS IN PRESENCE OF BEAM FIELDS

Figure 2 shows the time it takes for ions from the ionization event until they reach the detector. Without the space charge the travel time is around 180 ns, but when the space charge is included in the simulation, ions get additional kick which either accelerates them towards the detector or in the opposite direction. The final ion distribution on the detector is very spread and cannot be used for profile measurement, even when using much higher extraction fields.

Examples of ion trajectories, presented as their transverse position as a function of time, are shown in Fig. 3. After closer examination one can see that not only the kick from the bunch where they were produced plays role, but they are also affected by subsequent bunches. However, in this case, the effect of subsequent bunches on ion trajectories is rather small.

PROFILE DISTORTION IN ELECTRON-COLLECTING IPM

Because of their small mass, the electrons are extracted within a few nanoseconds. They spend less time in the high-field region, however the effect of this field on their dynamics is stronger.

One of the first ideas to counteract the profile distortion in IPM was to use magnetic field tuned such, that electrons

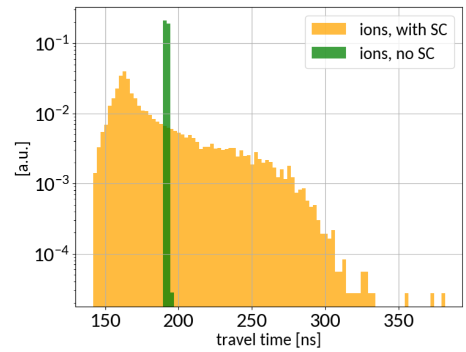

Figure 2: Travel time for ions, with and without space charge.

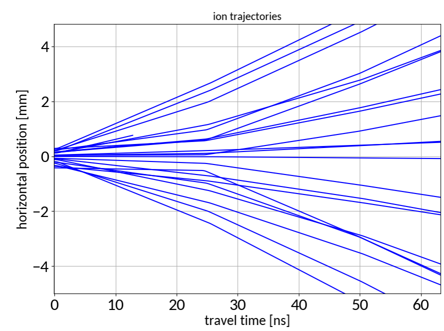

Figure 3: Examples of ion trajectories. The coordinate along the profile of positions are shown as a function of travel time.

would make exactly one revolution before reaching the detector. This idea was originally proposed in [10] to counteract the effect of initial electron velocities due to ionization. After single revolution electrons arrive, in the detector plane (x-z), to the location where they were created, independently of the component of momentum parallel to the detector (x-z). The magnetic field required in this approach is expressed in Eq. 2, where d_{beam} is the distance between the beam center and the detector.

$$B = \pi \sqrt{\frac{2 \cdot m_e \cdot E}{q_e \cdot d_{beam}}} \tag{2}$$

The main downside of this approach is a component of electron velocity perpendicular to the detector surface (y). This component affects the time of flight of the electron to the detector and for those electrons the Eq. 2 no longer holds. Figure 4 shows the original beam profile and the profiles observed in IPM with and without the space charge. Even without the space charge, small LHC beams cannot be measured using this approach.

Figure 5 shows the quality of the measured profile as a function of applied magnetic field. The "integer nmber of revolutions" - effect is visible as a series of local minima of the curves. Use of higher values of magnetic field show clear advantage, especially when the space charge is taken into account. Therefore, in most electron-based IPMs, the

ISBN: 978-3-95450-202-8 doi:10.18429/JACoW-HB2018-THA2WE02

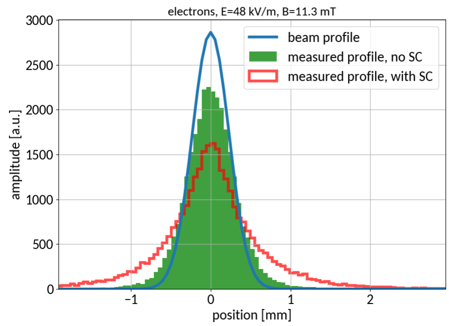

Figure 4: Simulated distortion of beam profile measured in LHC IPM.

magnetic fields of about 100 mT is used. Figure 6 shows the distortion of the registered beam profile for LHC IPM. In order to compensate this distortion a magnetic field of at least 0.6 T would be needed.

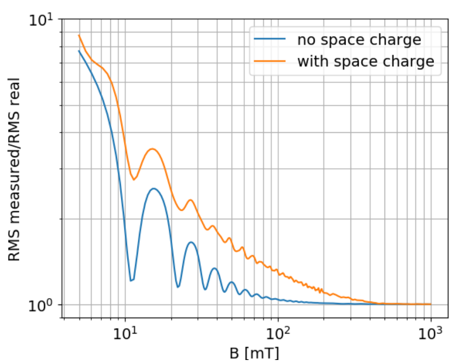

Figure 5: Dependency of the profile distortion on the IPM magnetic field.

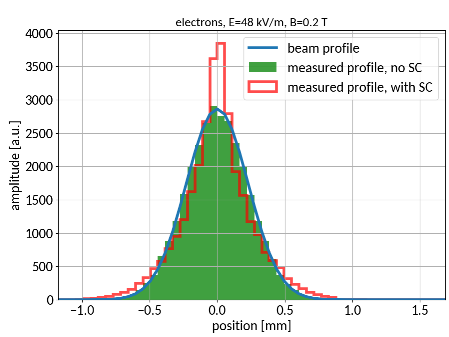

Figure 6: Simulated distortion of beam profile measured in LHC IPM.

The intuitive explanation of the profile deformation is that the electrons are pushed out of the area of the profile with large electric field towards the peak and towards the tails. Figure 7 shows vertical position of the electrons (y) as a function of the travel time. The electrons are trapped inside the bunch potential well until the bunch passes, therefore the deformation depends not only on the electric field in the position of ionization, but also on the time they spend trapped.

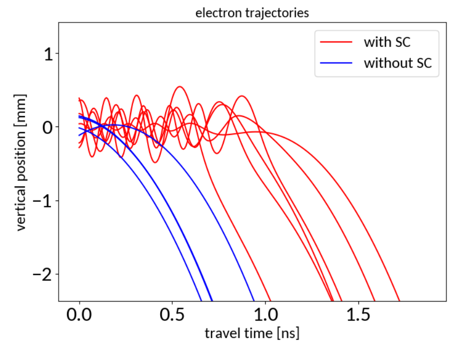

Figure 7: Simulated trajectories of the electrons. The vertical position as a function of time, zoomed to the first 1.5 ns after ionization.

PROFILE CORRECTION IN ELECTRON-COLLECTING, MAGNETIC IPM

Strong, large aperture magnets are big and expensive, therefore other ways to resolve profile deformation problem are discussed.

Electron Sieve

The idea of applying various deconvolution functions to components of the profile characterized by various gyroradius was investigated in [11, 12]. Theoretical results are promising, however practical realization of an "electron sieve" is difficult and has not been realized yet.

Obtaining Beam Width Using Machine Learning

Universal approximation theorem [13, 14] states that a feed-forward network, with a single hidden layer, containing a finite number of neurons, can approximate any continuous functions. The problem of profile distortion in IPM can be solved by a function which maps the distorted profile to real beam profile or beam width. Therefore, the artificial neural network (ANN) is a good tool to deal with the distortion.

In our first approach [15], a simple 2-layer ANN was used to find the original beam sigma. The network input was the distorted profile, bunch length and bunch population. The network was trained on a "grid" of 375 models and tested on models with beam size different than the the one used for training models. Optical point spread function was applied to the input profile and robustness of the network to noise was investigated.

The second approach [16] was focused on testing and comparison of various Machine Learning algorithms. Linear Regression, Ridge Regression, Kernel Ridge regression, Support Vector Machine Regression and ANN were compared. The algorithms were trained on 13500 random models and tested on a different sample of 2000 random beam

ISBN: 978-3-95450-202-8 doi:10.18429/JACoW-HB2018-THA2WE02

parameter sets. All models, also Linear Regression, performed well.

Linear Regression Linear regression model is the simplest of investigated algorithms. It can be expressed by Eq. 3.

$$\sigma_x = W^T \cdot x + b \tag{3}$$

where x is a vector containing input profile together with bunch length and charge, W is vector of weights and b is bias vector. W and b are found using fitting procedure, typically based on minimizing Mean Square Error.

Figure 8 shows a typical distribution of residuals obtained on validation sample after fitting procedure. The accuracy obtained on this sample is better than micrometer with submicrometer precision. This is already a very good result and it could be concluded that, in absence of significant noise, linear regression could be used for profile width reconstruction in IPM.

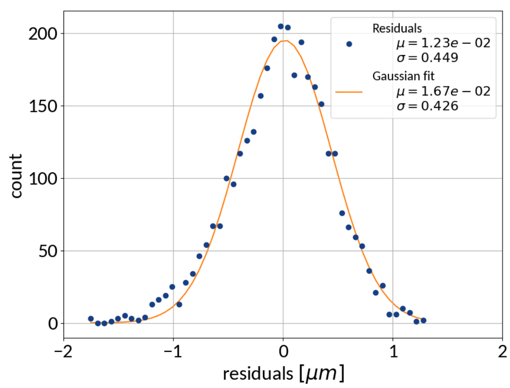

Figure 8: Residuals obtained with linear regression.

Profile Correction Using Neural Network

In order to reconstruct original beam profile, the neural network has been modified. The output of the network contains now not the beam sigma but the whole profile made of 98 fixed bins. The network has two hidden layers with arbitrary 88 neurons each.

The input and output profiles were normalized and centred. The network was trained and validated on the same samples of randomly chosen models as described before. The training converged after about 30 epochs.

In order to assess the quality of the profile reconstruction, a mean squared deviation (MSD) between the original profile and the distorted or corrected profile were calculated. Figure 9 presents the distribution of MSD for deformed and corrected profile for the validation sample. Improvement is clearly visible.

In the next step, the same ANN, trained on gaussian profiles only, was applied to beams with transverse profiles characterized by generalized gaussian and q-gaussian distributions. An example of MSD distribution for generalized

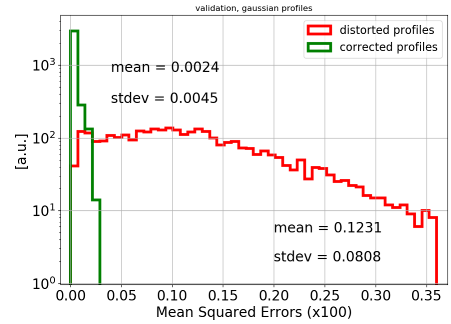

Figure 9: Mean Squared Deviation for gaussian profiles before and after correction.

gaussian profiles with $\beta = 3$ is shown in Fig. 10. A improvement is visible, even if the network was trained on gaussian profiles only, what might suggest that ANN learned about the way the space charge distorts the profiles and not about a particular transformation of gaussian profiles.

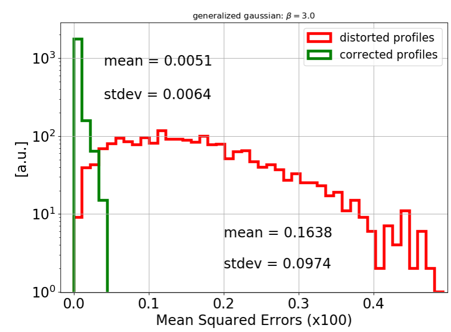

Figure 10: MSD for profiles with generalized gaussian distribution with $\beta = 3$: before and after correction.

An example of particularly distorted profile reconstruction for the generalized gaussian case is shown in Fig. 11. Similar procedure was tested successfully on other distributions.

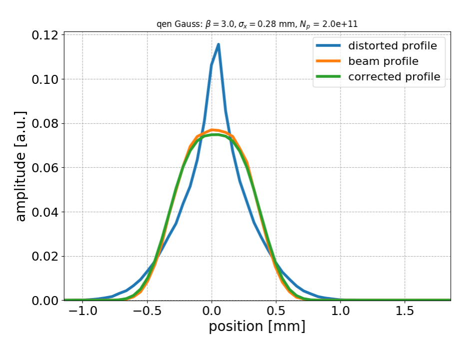

Figure 11: A case with particularly distorted profile. Original beam distribution is generalized gaussian with $\beta = 3$. ANN corrects the profile very accurately.

ISBN: 978-3-95450-202-8 doi:10.18429/JACoW-HB2018-THA2WE02

IPM FOR ULTRA LOW EMITTANCE BEAMS

Measurement of micrometer-scale beam size, like the one in Free Electron Lasers (XFEL), is a challenge for modern diagnostic methods. Here we want to draw attention to an approach which uses space-charge driven deformation of the profile to assess the maximum electric field of a bunch and therefore, when the bunch length and population can be independently measured, the bunch width. In some sense this idea is an alternative to the one presented in [17], which uses the measurement of ion energy.

Table 3: SwissXFEL Beam Parameters

Parameter	Range
particle type	electrons
σ_x	5-7 µm
σ_y	5 µm
σ_z	21 fs
N_{bunch}	230 pC
E_{beam}	5.8 GeV

In this example we use SwissXFEL beam parameters listed in Table 3. Figure 12 shows profiles obtained for various values of original beam size. The shape of the measured profile not only extends to measurable scales (*mm* instead of µm) but also strongly depends on the original beam size. This indicates that the measurement of the original beam width is viable.

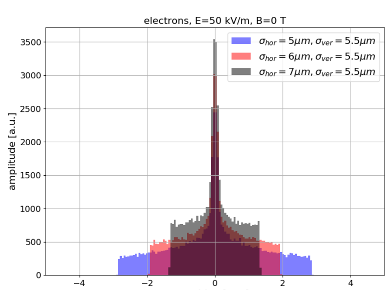

Figure 12: Beam profiles simulated for various SwissXFEL beam sizes.

CONCLUSIONS

Machine learning algorithms have proven to be very efficient in various applications. Here we succesfully used them for finding a correction to a complex dynamical process which affects beam profile measurement in Ionization Profile Monitors. Interestingly, an Artificial Neural Network trained on one type of beam profiles perform efficient correction on other types of profiles, suggesting that what network has really learned is the dynamics of the bunch field interaction with electrons and not a particular transformation of gaussian profile. Another interesting conclusion from the investigation is that even a much simpler, especially in interpretation, Linear Regression algorithm, performs as good as neural network in reconstructing the original beam width, suggesting that the deformation has a linear nature. At the end we propose to make use of profile distortion to measure size of micrometer-scale beams.

REFERENCES

[1] D. Bartkoski, "Analysis, Prototyping, and Design of an Ionization Profile Monitor for the Spallation Neutron Source Accumulator Ring", PhD diss., University of Tennessee, 2013.

[2] E. Thern, "Space-Charge Distortion in the Brookhaven Ionization Profile Monitor", in *Proc. PAC'87*, Washington DC, USA, Mar. 1987, p. 646.

[3] W. Graves, "Measurement of Transverse Emittance in the Fermilab Booster", PhD diss., University of Wisconsin, 1994.

[4] J. Amundson, J. Lackey, P. Spentzouris, G. Jungman, L. Spentzouris, "Calibration of the Fermilab Booster ionization profile monitor", *Phys. Rev. ST Accel. Beams* vol. 6, p. 102801, 2003.

[5] J. Egberts, "IFMIF-LIPAc Beam Diagnostics: Profiling and Loss Monitoring Systems", PhD diss., Universite Paris Sud, 2012.

[6] M. Sapinski *et al.*, "The First Experience with LHC Beam Gas Ionization Monitor", in *Proc. IBIC'12*, Tsukuba, Japan, Oct. 2012, paper TUPB61.

[7] M. Sapinski *et al.*, "Ionization Profile Monitor Simulations - Status and Future Plans", in *Proc. IBIC'16*, Barcelona, Spain, Sep. 2016, paper TUPG71.

[8] D. Vilsmeier, P. Forck, M. Sapinski, "A Modular Application for IPM Simulations", in *Proc. IBIC'17*, Grand Rapid, Michigan, USA, Aug. 2017, paper WEPCC07.

[9] S. Levasseur *et al.*, "Time-resolved Transverse Beam Profile Measurements with a Rest Gas Ionisation Profile Monitor Based on Hybrid Pixel Detectors", in *Proc. IPAC'18*, Vancouver, Canada, May 2018, paper WEPAL075.

[10] F. Hornsta, M. Trump, "A High Resolution Highly Sensitive Nonintercepting Beam Profile Monitor For The Los Alamos Meson Facility (LAMPF)", in *Proc. of Proton Linear Accelerator Conference*, Batavia, Illinois, USA, 1970.

[11] D. Vilsmeier, B. Dehning, M. Sapinski, "Investigation of the effect of beam space-charge on electrons in ionization profile monitors", in *Proc. HB'14*, East Lansing, MI, USA, November 2014, paper MOPAB42.

[12] D. Vilsmeier, "Profile distortion by beam space charge in Ionization Profile Monitors", CERN-THESIS-2015-035.

[13] G. Cybenko, "Approximations by superpositions of sigmoidal functions", *Mathematics of Control, Signals, and Systems*, vol. 2, no. 4, pp. 303-314, 1989, doi:10.1007/BF02551274

[14] K. Hornik, "Approximation Capabilities of Multilayer Feedforward Networks", *Neural Networks*, vol. 4, no. 2, pp. 251–257, 1991.

[15] R. Singh, M. Sapinski, D. Vilsmeier, "Simulation supported profile reconstruction with machine learning", in *Proc. IBIC'17*, Grand Rapid, Michigan, USA, Aug 2017, paper WEPCC06.

ISBN: 978-3-95450-202-8 doi:10.18429/JACoW-HB2018-THA2WE02

[16] D. Vilsmeier *et al.*, "Reconstructing Space-Charge Distorted IPM Profiles with Machine Learning Algorithms", in *Proc. IPAC'18*, Vancouver, Canada, May 2018, paper WEPAK008.

[17] R. Tarkeshian, J. L. Vay, R. Lehe, C. B. Schroeder, E. H. Esarey, T. Feurer, W. P. Leemans Phys. Rev. X 8, 021039.